AN IMPROVED HYDRODYNAMIC MODEL FOR PERCOLATION AND DRAINAGE DYNAMICS IN LEACH BED REACTORS

Laura Digan, Pierre Horgue, Gérald Debenest, Sébastien Pommier, Etienne Paul, Claire Dumas

AN IMPROVED HYDRODYNAMIC MODEL FOR PERCOLATION AND DRAINAGE DYNAMICS IN LEACH BED REACTORS

Laura Digan [1], Pierre Horgue [2], Gérald Debenest [2], Sébastien Pommier [1], Etienne Paul [1], Claire Dumas [1]

[1] LISBP, Université de Toulouse, CNRS, INRA, INSA, Toulouse, France
[2] INPT, UPS, IMFT (Institut de Mécanique des Fluides de Toulouse), Université de Toulouse, Allée Camille Soula, F-31400 Toulouse, France and CNRS, IMFT, F-31400 Toulouse, France

ABSTRACT: This study concerns the hydrodynamic modelling of percolation and drainage cycles in the context of solid-state anaerobic digestion and fermentation (VFA platform) of household wastes (HSW) in leach bed reactors. The focus was made on the characterization of the water distribution and hydrodynamic properties of the bed. A numerical model, set up with experimental data, highlighted that the simple dual-porosity model was not able to correctly reproduce all the hydrodynamic features and particularly the drainage dynamics. The model was improved by adding a reservoir (immobile) water fraction to macroporosity and allowed to correctly simulate dynamics. This model enabled to explain more precisely the water behaviour during percolation processes and these results should be useful for driving either solid-state anaerobic digestion or fermentation reactors.

Keywords: Solid-state anaerobic processes, leach-bed reactor, dual-porosity model, water retention, macroporous reservoir.

1. INTRODUCTION

Municipal solid wastes include a high organic fraction, especially coming from the residual household solid wastes. Organic wastes are usually transformed into biogas for heat and power Municipal solid wastes include a high organic fraction, especially coming from the residual household solid wastes.

Organic wastes are usually transformed into biogas for heat and power generation through anaerobic digestion but an alternative approach is carbon resource recovery. The LBR is a solid-state fermentation process in which the solid substrate remains static while the leachate is recirculated through the bed. This concept was initiated by Chynoweth et al. (1992) whose objective was to develop a process overcoming usual limitations encountered with high solid substrates. . Recirculation aims at maintaining a sufficient humidity in the bed, facilitating inoculation and mass diffusion between the solid and the flowing liquid (Jha et al. 2011; Francois et al. 2007; Lü et al. 2008; Stabnikova, Liu, and Wang 2008). The main highlighted advantages of this technology are: (i) its simple design and thus its relatively low cost (Dogan et al. 2009; Cysneiros et al. 2012; Yap et al. 2016) ; (ii) the improvement of bacterial activity due to wetting (Pommier et al. 2007), (iii) the acceleration of the first degradation stages, particularly acidogenesis (Francois et al. 2007). For VFAs production application, it has the advantage to enable simultaneous production and withdrawal of VFAs. In the LBR, a fraction of water is flowing between solid particles (macro-scale) while another fraction which is not flowing enables to wet the solid (micro-scale). VFAs are produced in contact of the substrate, in the micropores; then they are transferred to the macropores and can be recovered via the liquid flow (Veeken and Hamelers 2000). Dual-porosity models are usually proposed to simplify the description of water flow in a porous medium and has been previously used for modelling water behaviour in waste (Tinet et al, 2011, Han 2011). The model remains difficult to parametrize correctly since it requires exhaustive data such as relative permeability and retention curves (Gerke and Van Genuchten (1993)) . In the present study, the protocol and the dual-porosity model proposed by Shewani et al. (2015) were adapted and improved in order to better capture the experimental results. Waste beds were evaluated in terms of physical structure, and water flow through the wastes materials. .The model parameters were calculated from experimental data in order to compare the wastes, and to be able to predict wetting and drainage process to improve biological reactions.

2. EXPERIMENTAL MATERIAL AND METHODS

2.1. Waste materials

Two different wastes were used in this study: real wastes (from household wastes treatment centre Cavigny (Manche, France) and artificial household wastes. Real wastes were sorted to remove the largest pieces, before being introduced into the percolation column. Artificial household solid wastes (aHSW) were made from commercial products in order to mimic real household solid wastes. The composition was established according to a national household wastes characterization campaign (ADEME 2010). Once completely reconstituted, the aHSW were stored at ambient temperature for one week before use in order to simulate pre-fermented wastes such as the rHSW received. For percolation operations, no mechanical pre-treatment was carried out. The wastes were chemically characterized in terms of total solids (TS) and volatile solids (VS). For rHSW and aHSW samples, the drying was performed at 80°C until obtaining a constant mass, in order to prevent any loss of the waste's organic fraction by combustion (Stoltz et al. 2011). The VS content was determined for all wastes by ignition of previously dried samples at 550°C for 2 hours.

2.2. Experimental set-up

The experimental device for the hydraulic tests was the same as that used by Shewani et al. (2015) and composed of a steel column with a diameter of 0.40 m and a height of 0.75 m. A grid placed at the bottom of the column allowed to stop large solid particles from flowing out and clogging the exit nozzles. A drainage layer composed of gravel (size of 6 to 14 mm) was added under the rHSW and aHSW beds to facilitate the leachate flow and avoid clogging by particles. The gravel layer had a height of 0.04 m, representing 10% of the total bed height. The dry solids volume represented decreasingly 13.7, 7.1% m3.m-3 of total volume for respectively rHSW, aHSW. These values suggest a high total porosity fraction whatever the wastes considered (more than 86%). For feeding of the column, a tank containing water was connected to a peristaltic pump (Masterflex 77800-50).Water could be injected either through the bottom of the column (immersion phase for pre-wetting) directly from the pump to the central exit nozzle, or on top of the waste bed (percolation assays for hydrodynamic characterisation. In all cases, the liquid was drained through the five exit nozzles and collected into a drainage tank placed under the column. The feeding and drainage tanks were weighed continuously and the weights of injected and drained water were recorded every 20 seconds.

2.3. Hydraulic test protocol

The protocol for the hydraulic characterisation of the waste beds consisted in 5 successive steps :

immersion and drainage, percolation-drainage, bed compaction (to mimick a supplementary upper layer of waste exerting a pressure over the bed), immersion and drainage, and finally percolation-drainage step. The wastes bed height was measured all along the experiment. Settlement was supposed to be physical and not due to waste biodegradation. This assumption was made because: (i) no inoculum was introduced in the process and (ii) the total time of the experiment was relatively small compared to typical biodegradation times (one week). Thus, the dry solid mass was considered to remain constant (Shewani et al. 2015; Stoltz et al. 2011).

2.4. Calculations

From these measurements, the micropores volume (Vm) was calculated as the sum of initial water content with the injected volume which remained trapped. The dry solids volume (VDS) was estimated as the ratio between the dry solids mass (calculated with the total solids content measured prior to the experiment) and the dry solids particles density (ρSP). ρSP (kgTS.L-1) was computed as proposed by Agnew and Leonard (2003).

$$\rho_{SP} = \left(\frac{VS}{1.55} + \frac{(1 - VS)}{2.65}\right)^{-1}$$

Where VS is the volatile solids content expressed in kgVS.kgTS-1.
Finally, the macropores volume was deduced using the previously computed values VDS and Vm.

3. RESULTS AND DISCUSSION

3.1 HSW leach beds structure

The waste beds underwent water additions and compaction which modified their structure (total porosity, macropores, and micropores). The three main fractions (dry solids, micropores and macropores volumes) were quantified using the protocol described in ***Section 2.3*** at each step.

3.1.1. Wastes beds settlement and compressibility

A bed settlement occurred during the step 1 of the hydraulic characterization protocol (initial immersion and drainage). The rapid drainage of leachate under the effect of gravity creates a suction that drove the solid matrix towards the bottom , leading to the rearrangement (consolidation) of the bed. Understanding and measuring the effects of the settlement process on physical properties is crucial. They alter the flow behaviour and this has been already studied (Stoltz et al., 2010). For HSW, the first settlement might be mostly due to the 18 kg weights added on top of the beds to avoid flotation during step 1. From state CL 0 to CL 1, the bed porosity decreased from 86.3% to 81.1% for rHSW and from 92.9 to 88.9% for aHSW. No further settlement was observed over the first percolation series. At CL 2 stage, the total bed porosity (micro and macroporosity) accounted for 79.5% and 87.6% of total bed volume for rHSW and aHSW respectively. The compaction slightly amplified bed subsidence (step 4). For both HSWs, the bed volume did not decrease over the second percolation series. The total volume lost represented 33% and 43% of the initial bed volume for rHSW and aHSW respectively.

It is assumed that compressibility is characterized by the relative volume loss due on one hand to physical compression, and on the other hand to water drainage. The less the initial dry solids (or the more the initial void) volume fraction, the more the total volume loss. Compressibility was thus a waste-dependent parameter. Indeed, this parameter is driven by the waste composition (i.e. organic and mineral matter contents) (Chen et al. 2009), the elements size and their arrangement inside the matrix. At industrial scale, the bottom layer in the wastes bed is susceptible to compaction due to layers staking, and this could foster the reduction of leachate flow.

3.1.2. Wastes beds porosity evolution with compaction

The total porosity was globally high (from 79.4 to 86.3% for rHSW and from 87.6% to 92.9% for aHSW) at every stage of the experiment. After the first compaction (CL 1), the microporosity of the beds reached 56.8% and 48.0 % of the total volume for rHSW and aHSW respectively. At compaction level CL 2, microporosity fraction increased, representing 65.7% and 57.8% of total bed volume for rHSW and aHSW respectively. This increase of microporosity is made to the detriment of macroporosity fraction accounting for rHSW from 24.2% at CL 1 to 13.6% at CL 2, and for aHSW from 40.9 to 30.0% which suggests a bed rearrangement. Macropores volume was partially converted into microporous volume, which affects hydrodynamic properties of the medium. These results are consistent with those of Stoltz et al. (2011) who studied the evolution of pore size distribution with compression. They observed that mechanical compression of the solid material induced an increase of smaller pores and a decrease of larger pores. Since the fluid phases flow in the macropores, the reduction of macroporous volume may affect the water flow through the material (Reddy et al. 2009). At the same time, a gain in microporosity may increase the water retention capacity and could foster efficient contact (due to higher surface) between the substrate and the bacterial populations.

3.2. Behaviour of leach-bed with respect to water

3.2.1 Waste imbibition, micropores saturation

From the experimental masses of water injected in the leach bed and of leachate recovered, it is possible to calculate the amount of injected water retained in the wastes leach bed. ***Figure 2*** shows a typical evolution of the total water content over cumulated contact time. For the immersion-drainage step, the contact time was defined as the sum of injection time, rest time and the drainage time at which 90% of the total drained volume was collected. For each percolation-drainage cycle, the contact time was equal to the injection time added to the drainage time at which 90% of the total drained volume was collected. The cumulated contact time was thus the sum of each contact time (for a series of experiments).

$$Contact\ time = injection\ time + (rest\ time) + drainage\ time\ (90\%)$$

Successive injection and drainage phases led to a progressive increase of total water retained in the bed due to the imbibition of the waste. From the total water content evolution in time, the dynamic and static water contributions were dissociated using the values of water trapped in the solid waste bed after each percolation-drainage cycle. This allowed to evaluate the imbibition dynamics of the waste. Numerical simulations were then used to determine the filling rate of the microporosity α_{micro} (see ***Section 3.3.2***).

Following the microsaturation against total cumulated contact time shows that the time needed to reach 80% microsaturation is around 3 days which is relatively short compared to the characteristic time of anaerobic digestion process which generally runs over more than 20 days. However, acidogenic fermentation processes are operated for a few days only and the transient wetting period of 3 days could reduce the overall performance. During the compaction step, a small volume of water trapped in the microporosity flowed out of the waste beds due to the pressure exerted. At the same time, the microporosity volume increased (see ***Section 3.1.2***) and therefore, micropores saturation fell down from 100% and was over 89% for all waste beds After compaction, the filling behaviour was similar to the one observed before compaction.

3.2.2 Hydraulic conductivity, mobile water analysis

Hydraulic conductivity reflects the ability of a fluid to flow through a multiphase material (Richard et al. 2004). As described in previous works (Shewani et al. 2015; Gens Solé et al. 2011), the apparent (or effective) hydraulic conductivity (K_L) is the relationship between the volume of active water (that is flowing) inside the porous medium and the flow rate applied during percolation assays. An accurate characterisation of K_L allows to predict water volume used for transport. This volume is necessary to correctly predict water transfer between macro- and microporosity and solute transfer (such as VFA, see Shewani et al. (2017) (non characterized in this study). A good knowledge of water and flow distribution is then useful to adapt the leachate management strategy to the objective of the process (washing VFAs or increasing the concentration).

K_L is defined as the product of the intrinsic hydraulic conductivity (k_M) (which considers a saturated porous medium) and relative hydraulic conductivity (or permeability) ($k_{r,L}$) :

$$K_L = \underbrace{k_M}_{\text{intrinsic conductivity}} \cdot \underbrace{k_{r,L}}_{\text{relative conductivity}}$$

While k_M is an intrinsic function of medium parameters (porosity, tortuosity, pore size distribution and shape), $k_{r,L}$ is a function of medium parameters and dynamic variables such as macropores saturation (Wu 2016). The apparent conductivity K_L was directly deduced from the experimental flow rate applied. For both cases CL 1 and CL 2, the aHSW bed showed lower macropores saturations than rHSW which means that the conductivity of aHSW was higher and would be able to accept larger flow rate, without overflow on the reactor sides. This was particularly true in the rHSW-CL 2 case where pores were almost saturated for the highest flow rate (macropores saturation > 0.8) while it remains relatively unsaturated for aHSW (macropores saturation < 0.4). The fact that the aHSW bed can accept higher flow rates is possibly due to a more homogeneous structure related to the reconstitution of an artificial HSW. In a real case, as for rHSW, the wastes bed is heterogeneous, composed of elements having various sizes which may therefore show lower apparent hydraulic conductivity.

3.3. Modelling water behaviour in wastes leach-beds

Experiments allowed to observe water behaviour during percolation and drainage in wastes beds. By implementing a model, the objective was to describe more precisely the experimental observations, to predict water retention and water transfer and to correctly reproduce wetting and drainage processes. This can help in predicting the coupling of water transport phenomena with the biological reactions present during the fermentation/anaerobic digestion process.

3.3.1. Limitation of simplified dual-porosity model applied to household solid wastes

In a previous study (Shewani et al. 2015), a simplified capillary-free dual-porosity model was used to simulate water evolution in solid waste beds during series of percolation-drainage cycles.

In the present study, the simplified dual-porosity model was applied to real and artificial household wastes (rHSW, aHSW). The comparison between experimental and numerical simulation of dynamic water curves showed that whatever the wastes and compaction level considered, the water dynamics were not completely reproduced (see ***Figure 1***) especially the drainage part as observed by Shewani et al. (2015) for cattle manure. Indeed, the drainage dynamics depend both on relative permeability and water retention curves of the two porosities which are not handled in the simplified dual porosity model . The drainage dynamics, which were numerically too fast compared to the experimental observations, cannot be calibrated independently using only relative permeability curve. Moreover, the observation of the experimental drainage curves showed that whatever the flowrate applied, the drainage dynamics were similar. The similarity between the curves suggested that the “slow drainage part” is independent from the flow rate applied.

3.3.2. Implementing reservoir water to the mathematical model: description of the proposed model

In this work, the dual-porosity model was improved to obtain a more realistic and predictive model of the drainage process. For that purpose, it was hypothesized that during the percolation process a part of the water located inside macroporosity is not actually flowing but temporarily immobile in the internal cavities of the waste and hereby called: reservoir water. In the standard dual porosity model (Gerke and Van Genuchten 1993), when percolation occurs, the mobile water content increases such as the head pressure inducing water transfer from macro to micro-porosity (to equilibrate macro-head pressure with the micro-head pressure). When injection is stopped, the reduction of saturation in macro-porosity reduce macro-head pressure inducing a reverse water transfer from micro- to macro porosity. The system reaches the equilibrium when gravity forces in macro-porosity is balanced by capillary forces and when head pressure in both macro and micro-porosity are at the equilibrium (which generally correspond to high level of saturation in micro-porosity and low level in macro-porosity since capillary effects are higher in micropores). In the proposed model, the micro-porosity of usual dual-porosity model is dissociated into two porosities, (i) the static water which remains trapped even after drainage and (ii) the reservoir which is trapped temporarily when mobile water is flowing. This dissociation is made possible by considering that the filling and drainage time of the mobile water are negligible compared to that of the reservoir water.

The 3 conservation equations numerically related to saturation (S) are:

$$\underbrace{\epsilon_{Macro}\frac{\partial S_{Macro}}{\partial t}}_{\text{Mobile macroporosity saturation}} + \underbrace{\nabla . U_{water}}_{\text{Mobile water transport}} = \underbrace{-q_{Macro,res}}_{\text{Mobile - reservoir exchange}} - \underbrace{q_{micro}}_{\text{Mobile -static exchange}} \quad \text{(Equation 1)}$$

$$\underbrace{\epsilon_{Macro,res}\frac{\partial S_{Macro,res}}{\partial t}}_{\text{Macroporous reservoir saturation}} = \underbrace{q_{Macro,res}}_{\text{Mobile - reservoir exchange}} \quad \text{(Equation 2)}$$

$$\underbrace{\epsilon_{micro}\frac{\partial S_{Micro}}{\partial t}}_{\text{Micro}pores\ saturation} = \underbrace{q_{micro}}_{\text{Mobile-static exchange}} \quad \text{(Equation 3)}$$

Where ϵ_{Macro}, $\epsilon_{Macro,res}$ and ϵ_{micro} are the “mobile” macroporosity, the “reservoir” macroporosity and the microporosity fractions, respectively.

A first order model is applied for the mobile-reservoir exchange term $q_{Macro,res}$:

$$q_{Macro,res} = \begin{cases} \underbrace{\alpha_{res,charge}}_{\text{Exchange coefficient for reservoir charge}} \left(1 - \underbrace{S_{Macro,res}}_{\text{Macroporous reservoir saturation}}\right) \text{if charge} \\ \underbrace{-\alpha_{res,discharge}}_{\text{Exchange coefficient for reservoir discharge}} \cdot \underbrace{S_{Macro,res}}_{\text{Macroporous reservoir saturation}} \quad \text{if discharge} \end{cases} \quad \text{(Equation 4)}$$

And the mobile-static exchange term q_{micro} (exclusively in charge since water remains trapped in microporosity):

$$q_{micro} = \underbrace{\alpha_{micro}}_{\text{Exchange coefficient for micropores charge}} \left(1 - \underbrace{S_{micro}}_{\text{Micropores saturation}}\right) \quad \text{(Equation 5)}$$

$\alpha_{res,charge}$ and $\alpha_{res,discharge}$ (s^{-1}) stand respectively for the exchange coefficient between “mobile” and “reservoir” macroporous water during the charge and discharge cycles. α_{micro} is the exchange coefficient between “mobile” macroporous water and static water. $S_{Macro,res}$ and S_{micro} ($m^3.m^{-3}$) are the macroporous reservoir and micropores saturations, respectively.

The water-mobile velocity U_{water} ($m.s^{-1}$) is modelled and computed using the generalized Darcy’s law with a classical Brooks and Corey (power law) model for relative permeability (Brooks and Corey 1964):

$$\underbrace{U_{water}}_{\text{Mobile water velocity}} = \underbrace{K_L}_{\text{Hydraulic conductivity}} \cdot \underbrace{S_{Macro}^{p}}_{\text{Mobile macroporosity saturation}} \qquad \text{(Equation 6)}$$

Where K_L (m.s^{-1}) is the hydraulic conductivity of the porous medium, S_{Macro} (m^3.m^{-3}) is the mobile macroporous water saturation, and p is the Brooks and Corey coefficient. The Brooks and Corey parameters K_L and p are evaluated in order to fit experimental points available. This allows the evaluation of the mobile water content (macrosaturation) for a given flow rate during numerical simulation. The Brooks and Corey model is one of the main models used for permeability (and therefore hydraulic conductivity) correlations. Stoltz et al. (2011) also calibrated this type of model with real municipal solid wastes for drainage retention properties and concluded that it was applicable to these wastes.

For a given waste composition, all the parameters need to be characterized by experimental measurements: the 3 porosities (ϵ_{Macro}, $\epsilon_{Macro,res}$ and ϵ_{micro}), the 3 exchange rates ($\alpha_{res,charge}$, $\alpha_{res,discharge}$ and α_{micro}) and the coefficients (K_L and p) for the relative permeability law. An 8-parameter optimization is complex to set up and would require excessive computation times. Moreover, characteristic times between processes are different (imbibition of the waste is much slower than filling/emptying the reservoir part and the mobile saturation variations are fast and considered as instantaneous) which allows a progressive parametrisation as described in ***Section 3.3.3***.

3.3.3. Application of improved dual-porosity model to HSW

In this part, it is considered that static/dynamic water decomposition has been delineated in independent experiments as described in ***Section 3.2.1*** (ϵ_{micro} and α_{micro} are already characterized) and only the dynamic water evolution (which cannot be reproduced by simplified model) is studied. To determine the reservoir macroporosity, the experimental drainage curves are time-shifted and plotted such as initial time corresponds to the moment when injection is stopped.

In these conditions, the drainage curves are similar for all flow rates tested, i.e. starting with a quasi-instantaneous drainage of a part of the water content followed by an inflection of the curve which indicates the beginning of the slower drainage part. The distinction between fast and slow drainage part is purely conceptual and cannot be determined precisely. From the experimental data, we determine the beginning of the slower drainage as the moment when the drainage flow-rate measurement reaches the experimental precision (0.01 L/min) which corresponds in our case to 10% of the maximal drainage flow rate measured. In this study, the evaluated reservoir water content is equal to 2.28 L ±0.12. The reservoir porosity $\epsilon_{Macro,res}$ is then directly computed from reservoir water volume evaluated. ϵ_{Macro} is simply deduced from the already known microporosity and solid fractions. This hypothesis allows the decomposition of dynamic water into mobile and reservoir macroporous water.

From this decomposition, the Brooks and Corey parameters (K_L and p) can be directly fitted using the series of plateaus (as described in ***Section 3.2.2***) while the charge $\alpha_{res,charge}$ and discharge $\alpha_{res,discharge}$ rate are calibrated using numerical simulations.

In ***Figure 2***, a comparison of dynamic water retention from experiments and numerical simulations are presented for both rHSW and aHSW at two compaction levels (CL 1 and CL 2). The comparison between simulated and experimental data reveals a quite good representation of the percolation and drainage dynamics whatever the state of the beds and the wastes considered.

The general behaviour for both wastes are similar with the same charge rate of the reservoir macroporosity ($\alpha_{res,charge}$=1.29 day^{-1}). The discharge of reservoir macroporosity was a little bit slower for rHSW $\alpha_{res,discharge}$=0.26 day^{-1} than for aHSW $\alpha_{res,discharge}$=0.35 day^{-1}. These observations were consistent with the higher hydraulic conductivity for aHSW than rHSW (53.1 cm.h^{-1} and 43.4 cm.h^{-1} respectively).

Note that for both wastes, the second percolation cycle at low flow rate (6L/h) shows higher water content than for the last percolation cycle although the flow rate is identical (***Figure 8***). This highlights that partial wetting of the substrate has a non negligible influence on dynamic saturation during the first phase of imbibition

Compaction seems to have no influence on the charging rate of reservoir water whatever the wastes considered (rHSW or aHSW). However, it affects discharge rate of reservoir macroporous water in the case of aHSW with a decrease from 0.35 to 0.17 day^{-1}. Compaction involved a rearrangement of the bed structure that might make the reservoirs drainage slow. This was not the case for rHSW beds.

4. CONCLUSIONS

In this study, the various water dynamics occurring during percolation and drainage through solid wastes leach-beds were investigated for different types of wastes under two compaction levels. The simplified capillary-free dual-porosity model was not able to completely reproduce the water dynamics, particularly the drainage dynamics. Thus the model has been extended by adding an immobile (reservoir) fraction to macroporosity which to calibrate the model using only water content measurements without retention curves.

An improved experimental procedure was developed to correctly evaluate the effective parameters described in the model. The model enabled to correctly simulate dynamics for all configurations and to explain more precisely the behaviour of leachate and water during leaching processes. The new description of water flow highlighted the presence of water in macroporous reservoirs. It is important for leachate recirculation strategy in wastes digestion context.

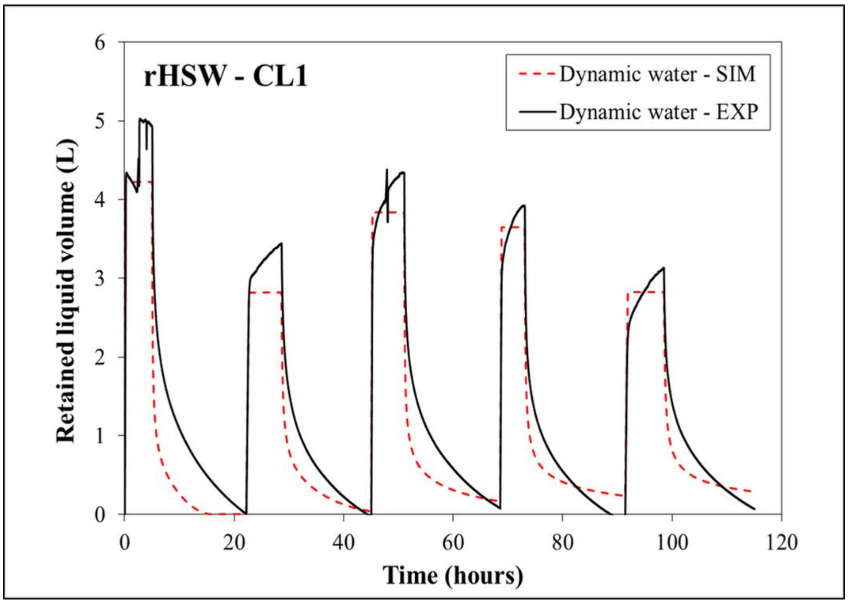

Figure 1. An example of dynamic water modelling with classical porous medium model.

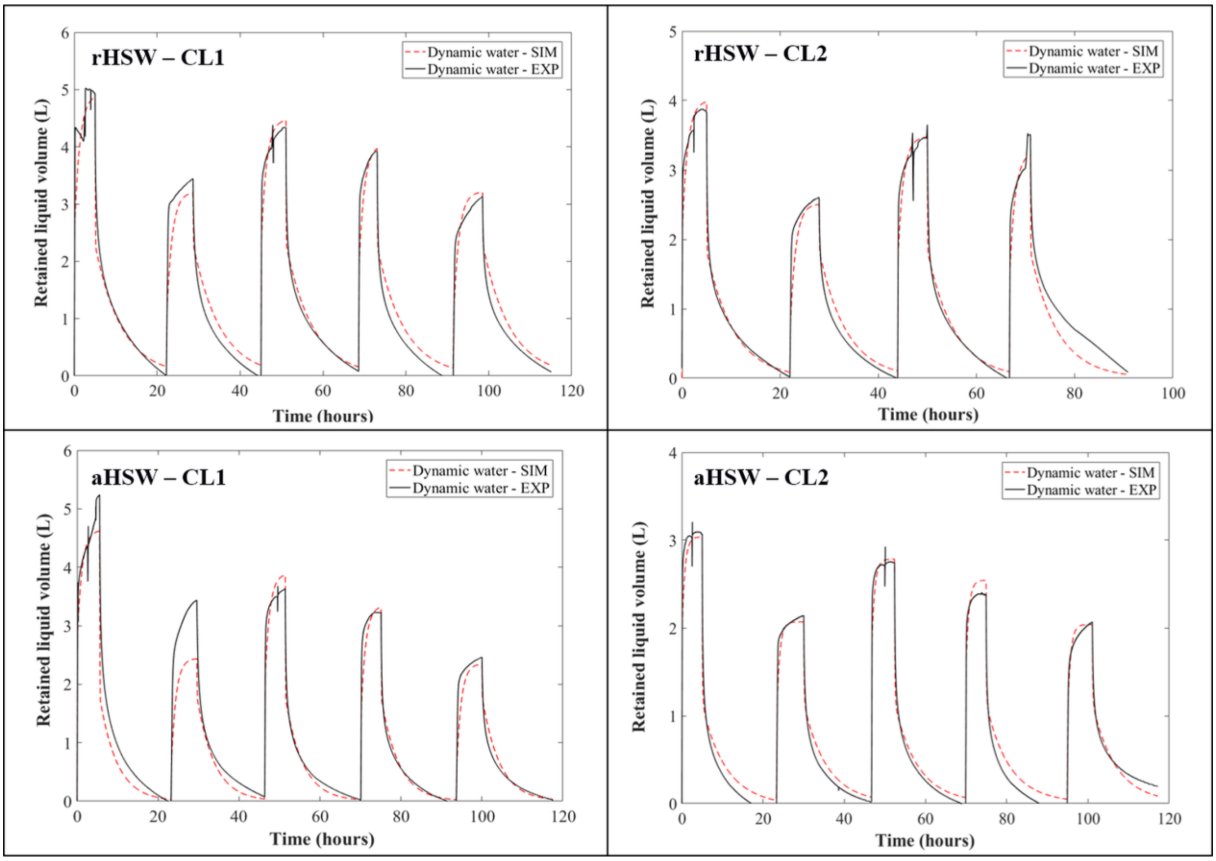

Figure 2. Measured and simulated evolution of dynamic water retention over a percolation-drainage series for rHSW and aHSW. Dynamic water is plotted for all the different percolation flow rates.

AKNOWLEDGEMENTS

This work was supported by the project RECOWER funded by the Carnot Institute 3BCAR. The authors want to acknowledge French research ministry for Laura Digan PhD financial support. The authors would like to acknowledge also Anil Shewani, Zhe Li, Matthieu Peyre-Lavigne, Mansour Bounouba, Evrard Mengelle, Simon Dubos, Chantha Kim, Michel Mauret and Xavier Lefebvre for their numerous contributions to the work.

REFERENCES

ADEME. La composition des ordures ménagères et assimilées en France. Angers: ADEME Editions, 2010.

Agnew, J. M., and J. J. Leonard. 2003. 'The Physical Properties of Compost'. Compost Science & Utilization 11 (3): 238–64.

Brooks, R.H., Corey, A.T., 1964. Hydraulic properties of porous media. Hydrology Papers. Colorado State University.

Chen, Y. M., Tony L. T. Zhan, H. Y. Wei, and H. Ke. 2009. 'Aging and Compressibility of Municipal Solid Wastes'. Waste Management 29 (1): 86–95. https://doi.org/10.1016/j.wasman.2008.02.024.

Cysneiros, Denise, Charles J. Banks, Sonia Heaven, and Kimon-Andreas G. Karatzas. 2012. 'The Effect of PH Control and "Hydraulic Flush" on Hydrolysis and Volatile Fatty Acids (VFA) Production and Profile in Anaerobic Leach Bed Reactors Digesting a High Solids Content Substrate'. Bioresource Technology 123 (November): 263–71. https://doi.org/10.1016/j.biortech.2012.06.060.

Dogan, E., T. Dunaev, T. H. Erguder, and G. N. Demirer. 2009. 'Performance of Leaching Bed Reactor Converting the Organic Fraction of Municipal Solid Waste to Organic Acids and Alcohols'. Chemosphere 74 (6): 797–803. https://doi.org/10.1016/j.chemosphere.2008.10.028.

Francois, V., G. Feuillade, G. Matejka, T. Lagier, and N. Skhiri. 2007. 'Leachate Recirculation Effects on Waste Degradation: Study on Columns'. Waste Management 27 (9): 1259–72. https://doi.org/10.1016/j.wasman.2006.07.028.

Gens Solé, Antonio, Beatriz Vállejan, M. Sánchez, Cristophe Imbert, Maria Victoria Villar, and Maarten Van Geetl. 2011. 'Hydromechanical Behaviour of a Heterogeneous Compacted Soil: Experimental Observations and Modelling'. Geotechnique 61 (5): 367–386.

Jha, A. K., J. Li, L. Nies, and L. Zhang. 2011. 'Research Advances in Dry Anaerobic Digestion Process of Solid Organic Wastes'. African Journal of Biotechnology 10 (64): 14242–53.

Lü, F., P. J. He, L. P. Hao, and L. M. Shao. 2008. 'Impact of Recycled Effluent on the Hydrolysis during Anaerobic Digestion of Vegetable and Flower Waste'. Water Science and Technology 58 (8): 1637–43. https://doi.org/10.2166/wst.2008.511.

Pommier, S., D. Chenu, M. Quintard, and X. Lefebvre. 2007. 'A Logistic Model for the Prediction of the Influence of Water on the Solid Waste Methanization in Landfills'. Biotechnology and Bioengineering 97 (3): 473–82. https://doi.org/10.1002/bit.21241.

Reddy, Krishna R., Hiroshan Hettiarachchi, Naveen Parakalla, Janardhanan Gangathulasi, Jean Bogner, and Thomas Lagier. 2009. 'Hydraulic Conductivity of MSW in Landfills'. Journal of Environmental Engineering 135 (8): 677–83. https://doi.org/10.1061/(ASCE)EE.1943-7870.0000031.

Richard, Tom L., Adrie H. M. Veeken, Vinnie de Wilde, and H. V. M. (Bert) Hamelers. 2004. 'Air-Filled Porosity and Permeability Relationships during Solid-State Fermentation'. Biotechnology Progress 20 (5): 1372–81. https://doi.org/10.1021/bp0499505.

Shewani, Anil, Pierre Horgue, Sébastien Pommier, Gérald Debenest, Xavier Lefebvre, Sophie Decremps, and Etienne Paul. 2017. 'Assessment of Solute Transfer Between Static and Dynamic Water During Percolation Through a Solid Leach Bed in Dry Batch Anaerobic Digestion Processes'. Waste and Biomass Valorization, July. https://doi.org/10.1007/s12649-017-0011-1.

Shewani, Anil, Pierre Horgue, Sébastien Pommier, Gérald Debenest, Xavier Lefebvre, Emmanuel Gandon, and Etienne Paul. 2015. 'Assessment of Percolation through a Solid Leach Bed in Dry Batch Anaerobic Digestion Processes'. Bioresource Technology 178 (February): 209–16. https://doi.org/10.1016/j.biortech.2014.10.017.

Stabnikova, Olena, Xue-Yan Liu, and Jing-Yuan Wang. 2008. 'Anaerobic Digestion of Food Waste in a Hybrid Anaerobic Solid–liquid System with Leachate Recirculation in an Acidogenic Reactor'. Biochemical Engineering Journal 41 (2): 198–201. https://doi.org/10.1016/j.bej.2008.05.008.

Stoltz, Guillaume, Jean-Pierre Gourc, and Laurent Oxarango. 2010. 'Liquid and Gas Permeabilities of Unsaturated Municipal Solid Waste under Compression'. Journal of Contaminant Hydrology 118 (1–2): 27–42. https://doi.org/10.1016/j.jconhyd.2010.07.008.

Stoltz, Guillaume, Anne-Julie Tinet, Matthias J. Staub, Laurent Oxarango, and Jean-Pierre Gourc. 2011. 'Moisture Retention Properties of Municipal Solid Waste in Relation to Compression'. Journal of Geotechnical and Geoenvironmental Engineering 138 (4): 535–543.

Tinet, A-J., L. Oxarango, R. Bayard, H. Benbelkacem, G. Stoltz, M.J. Staub, and J.-P. Gourc. 2011. 'Experimental and Theoretical Assessment of the Multi-Domain Flow Behaviour in a Waste Body during Leachate Infiltration'. Waste Management 31 (8): 1797–1806. https://doi.org/10.1016/j.wasman.2011.03.003.

Veeken, A.H.M, and B.V.M. Hamelers. 2000. 'Effect of Substrate-Seed Mixing and Leachate Recirculation on Solid State Digestion of Biowaste'. Water Science and Technology 41 (3): 255–62.

Viéitez, E. R, and S Ghosh. 1999. 'Biogasification of Solid Wastes by Two-Phase Anaerobic Fermentation'. Biomass and Bioenergy 16 (5): 299–309. https://doi.org/10.1016/S0961-9534(99)00002-1.

Wu, Yu-Shu. 2016. 'Multiphase Fluids in Porous Media'. In Multiphase Fluid Flow in Porous and Fractured Reservoirs, 15–27. Elsevier. https://doi.org/10.1016/B978-0-12-803848-2.00002-7.

Yap, S.D., S. Astals, P.D. Jensen, D.J. Batstone, and S. Tait. 2016. 'Pilot-Scale Testing of a Leachbed for Anaerobic Digestion of Livestock Residues on-Farm'. Waste Management, March. https://doi.org/10.1016/j.wasman.2016.02.031.